International Journal of Engineering, Mathematical and Physical Sciences
ISSN: 2517-9934
Vol:6, No:10, 2012

Optimization of Supersonic Ejector via Sequence-Adapted Micro-Genetic Algorithm

Kolar Jan, and Dvorak Vaclav

***Abstract*—**In this study, an optimization of supersonic air-to-air ejector is carried out by a recently developed single-objective genetic algorithm based on adaption of sequence of individuals. Adaptation of sequence is based on Shape-based distance of individuals and embedded micro-genetic algorithm. The optimal sequence found defines the succession of CFD-aimed objective calculation within each generation of regular micro-genetic algorithm. A spring-based deformation mutates the computational grid starting the initial individualvia adapted population in the optimized sequence. Selection of a generation initial individual is knowledge-based. A direct comparison of the newly defined and standard micro-genetic algorithm is carried out for supersonic air-to-air ejector. The only objective is to minimize the loose of total stagnation pressure in the ejector. The result is that sequence-adopted micro-genetic algorithm can provide comparative results to standard algorithm but in significantly lower number of overall CFD iteration steps.

***Keywords*—**Grid deformation, Micro-genetic algorithm, shape-based sequence, supersonic ejector.

I. Introduction

IN the framework of evolutionary computation, genetic algorithms (GAs) have become extremely popular in the course of years. Other evolutionary algorithms, frequently used in the optimization community are simulated annealing, particle swarm optimization algorithms and ant colony algorithms, just to name a few. As it is well known, genetic algorithms are mimicking the natural evolution via applying simple evolutionary operators to a set of populations of individuals (design or decision vectors), namely selection, cross over and mutation. After letting these to act on the population for sufficiently many generations, the evolution eventually gets to the optimum. In the case of single objective, this would be a single member of the population. In this study, the supersonic ejector underlies the evolution process to gain better performance.

Supersonic ejectors are simple mechanical components shown in the Fig. 1, which generally allow performing the mixing and/or the recompression of two fluid streams. The fluid with the highest total energy is the motive or primary stream (p_{01}), while the other with lowest total energy is the secondary or induced stream [1]. In our case the induced stream comes directly from atmosphere. Operation of such system is also quite simple: the motive (high pressure) stream flows through a convergent divergent nozzle to reach the supersonic velocity. By an entrainment –induced effect, the secondary stream is drawn into the flow and accelerated. Mixing and recompression of the resulting stream than occurs in mixing chamber, where complex interactions take place between the mixing layer and shocks [2], [3]. In other words, there is mechanical energy transfer from the highest to the lowest energy level, with a mixing pressure lying between the motive and induction pressure.

Kolar Jan. is with the Technical University of Liberec, Studentska 2, Liberec 461 17, Czech Republic, (e-mail: jan.kolar1@tul.cz).

Dvorak Vaclav. is with the Technical University of Liberec, Studentska 2, Liberec 461 17, Czech Republic, (e-mail: Vaclav.dvorak@tul.cz).

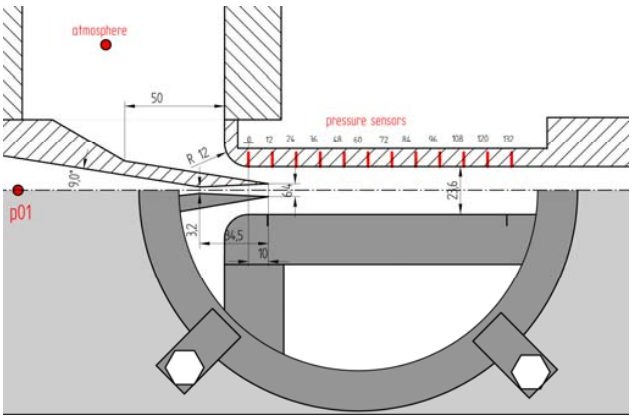

Fig. 1 Supersonic air-to-air ejector scheme of the initial design

The goal of supersonic air-to-air ejector optimization lies in the minimizing of stagnation pressure loses. These loses are caused by mixing processes, viscosity effects as turbulence, shear stress and compressibility effects as shocks and their interactions just to name a few [2].

Experimental devices for basic research in a field of supersonic or transonic speed need to be designed very carefully to avoid above mentioned effects as much as possible. Primary nozzle of the supersonic air-to-air ejector is one of those parts, whose quality typically determines properties of whole device. Both streams coming into the ejector are ideally shock and flow separation free. Beyond this, it should provide flow field without large gradients of flow variables and with uniform velocity profile at the exit.

There were numerous experiments carried out with the aim of ejector shown in the Fig.1. Some of them are mentioned in [3]-[5]. The best settings of CFD solver was found at the base of comparisons of computed and Schlieren pictured flow fields in previous work [3]. Various regimes were investigated experimentally and numerically. During these simulations, very low solver stability occurred due to high nonlinearity of problem. This instability does not allow using a standard CFD initialization, instead an interpolation from the afore-computed individual needs to be used.

II. Standard and Adapted Sequence Micro Genetic Algorithms

There is a flowchart of standard genetic algorithm used for CFD simulations in the Fig 2.

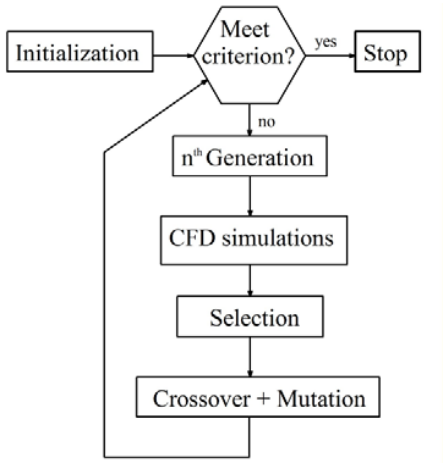

Fig. 2 Flowchart of standard single-objective GA

The standard algorithm was modified to avoid all inconveniences cited in the introduction to that shown in the Fig. 3.

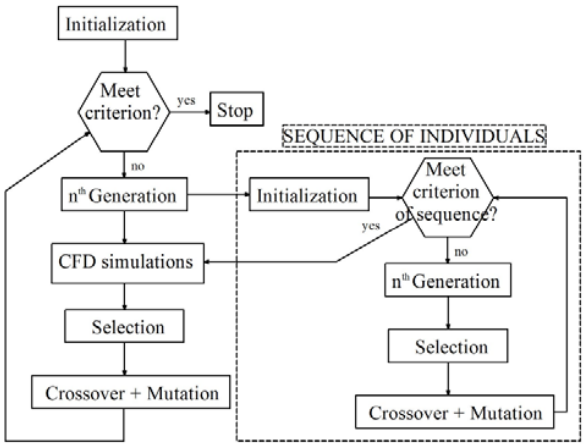

Fig. 3 Flowchart of single-objective GA with sequence adaptation

Routine presented in the Fig. 3 does not evaluate objective for vectors in random orderas mentioned in [6]. Instead the optimal sequence is followed for mutual deformation of shapes (vectors from design space), needed to deform the nozzle shape over all selected vectors

$$\boldsymbol{V_i}=(P1_i,P2_i,P3_i,P4_i,P5_i),\ where$$

$$for\ \forall i\ is\ V_i \in (design\ space)\ and\ i=0,1,2,\ldots,\ SIZE \qquad (1)$$

is followed. The "*SIZE*" has meaning of the size of population. Unfortunately, finding of optimally adapted sequence (OAS) is not from those of trivial task as described by Breitkopf in [6], Hynek in [7] and Holland in [8]. This task is identical to well-known traveling salesman problem (TSP). Where given a list of K cities and their pair wise distances (deformation), the task is to find the shortest possible tour that visits each city exactly once. In this task the salesman has to visit cities of given locations, starting from his city and returning back. In the theory of computational complexity, the decision version of TSP belongs to the class of NP-complete problems. The only approach able to improve objective are heuristic algorithms. One of the most efficient is the genetic algorithm (GA) firstly introduced by Holland [8]. Several modifications of standard approach is used to improve convergence to global optimum and help objective to improve.

One of the most significant tasks in GA optimization is the methodology of coding the individuals. As the GA further works with individuals represented by its chromosomes and all operators are applied to theme, technique of individual coding has a significant impact to EA advance as mentioned by Hynek in [7] and Zelinka in [9]. If there is no suitable coding applied, even an infinitesimal change of chromosome code may have large impact to the objective function. Typical example is a chromosome handled in binary code, where even one binary-unite-change in number $(11010110)_2$=214 produces the $(10010110)_2$=150. The GA than betrays itself. We decided to use parameter based code, where the chromosome gets value of parameters as a real number.

Selection of individuals for further evolution is based on fitness proportionate selection with its modification: stochastic universal sampling. More detailed view can is taken by Hynek in [8].

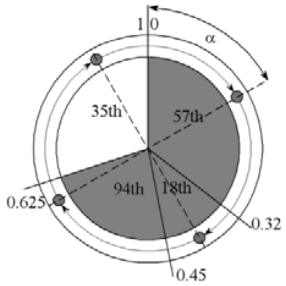

Fig. 4 Stochastic universal sampling

In the Fig. 4, there is an example of selection of four individuals (balls). In standard GA this has the meaning of selection of real individual (ejector shape) in optimization of sequence, the individual has meaning of given shape sequence (set of ejector shapes mutating from initial one to final one). The individual is selected when the randomly generated number α is such, that

$$\bar{f}_{i-1} < \alpha \le \bar{f}_i \_ where \_ i = 1,2,\ldots, SIZE\ , \qquad (2)$$

where the SIZE is the size of population, $f$is the individual fitness and $\bar{f}_i$ is defined as follows

$$\bar{f}_i = \sum_{j'=1}^{i} \frac{f_i}{\sum_{k=1}^{SIZE} f_k},\ where \qquad i = 1,2,\ldots,SIZE. \qquad (3)$$

One of the most effective recombination operators for TSP is the edge recombination crossover (ERX). In this method the only one child, is reproduced from parent's couple.Its chromosome path is combination of mothers and fathers

chromosome part of path. See more details in [7]-[9].

Optimized sequence is defined via the shape-based similarity query which defines the similarity of shapes or trajectory in a space. Most of database systems adopt the Euclidean distance of two data sequences for analysis, where each has n values. Similarity is given by the Euclidean distance between vectors in $\mathbf{R}^2$. In Yanagisawa [10], there are two data series $c = \langle w_1, w_2, \ldots, w_n \rangle$, $c' = \langle w'_1, w'_2, \ldots, w'_n \rangle$. Then, the distance $D(c,c')$ is defined as follows

$$D(c,c') = \sqrt{(w_1 - w'_1)^2 + \cdots (w_n - w'_n)^2}. \quad (4)$$

Based on this definition, we consider the spatial shape-based similarity for curves or planes. In our case, data series represent y-coordinate of two-dimensional ejector shape. X-coordinate is represented by the index of thei^{th} value. This is valid for consistent data-sampling of both, series c and c'. For non-consistent data sampling we need to define location vector ***x*** instead of single coordinate as shown in the figure 3.

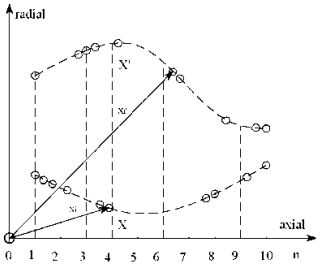

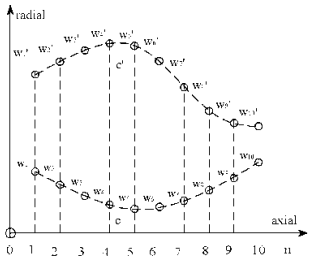

Fig. 5(a) Inconsistent data sampling. Location vectors in $\mathbf{R}^2$

Fig. 5(b) Consistent sampling

Equation (4) is an extension for location vectors, where the spatial definition of curve is given by the location vector series. If each location vector *x*is a vector in space $\mathbf{R}^2$ andvectors series are $X = \langle x_1, x_2, \ldots x_n \rangle$, $X' = \langle x'_1, x'_2, \ldots x'_n \rangle$, the distance of vector series is defined as follows

$$D(X,X') = \sqrt{D(X_1,X'_1)^2 + + \cdots + D(X_n,X'_n)^2}. \quad (5)$$

III. Problem Parameterization

As the first step of optimum design finding, only the primary (driving) nozzle was optimized, while the rest of ejector remains the same. This was used mainly for testing of newly formed routine. Problem was defined into design space of five parameters seen in the Fig.6, P1, P2, P3, α1, α2.

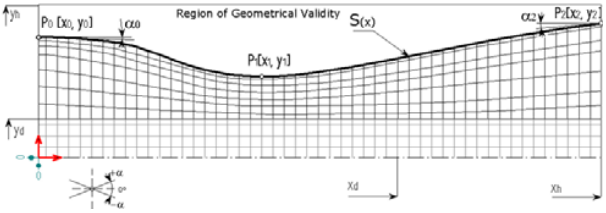

Fig. 6 Scheme of driving nozzle. It's driving spline and mesh

Example of adapted sequence of five nozzle shapes is shown in the Fig. 7.

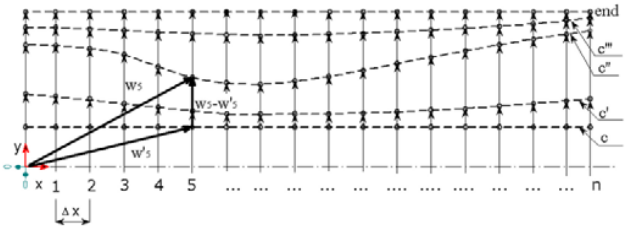

Fig. 7 Example of optimized mutation of nozzle boundary nodes

IV. CFD Simulations

We used the commercial code FLUENT to solve 2D RANS equations with the $k-\omega$ SST by Finite Volume Technique [10], [11] and [12]. For all equations, convective terms are discretized using a second-order upwind scheme; inviscid fluxes are derived using a second order flux splitting achieving the necessary upwinding and dissipation close to shocks. We choose the density based solver with the implicit formulation. Diffusion terms are always cast into a central difference form. The criterion for assessing convergence was based on the root mean square of the density residues expressed by

$$R(\xi) = \left[\sum_{i=1}^{M} \left(\frac{\partial \xi}{\partial t}\right)_i^2\right]^{1/2} \quad (6)$$

where M is the number of grid points and ξ is the variable considered to check (mass, energy, momentum, etc.). Generally, computations are stopped when residuals fall below $1x10^{-6}$ and when the solution is was no longer changing. In addition, at convergence, the mass imbalance is checked on each inlet and outlet boundaries. All mentioned requirements were meet in with Courant-Friedrichs-Lewy (CFL) number set to 1 [11]. Boundary conditions were set to pressure inlet/outlet with non-reflecting boundary condition (outlet pressure at infinity). Turbulent intensity was set to 8 %at the primary nozzle inlet and to 2 % at the secondary nozzle intake. Both, gauge total pressure p_{01}=175 kPa and the outlet gauge pressure $p_{exit} = -77\ kPa$ were set to design regime of initial shape. Symmetric computational domain split by the symmetry boundary condition consists of $4.5E^5$ quadrilateral elements with original mesh size 0.2 mm. We defined the grid-gradual boundary layer in ten levels from the size of $5E^{-3}$ mm in wall adjacent cells to the free stream value.

The two-dimensional Reynolds Averaged Navier-Stokes equations were completed by k-ω SST eddy viscosity model. The turbulence kinetic energy k and the specific dissipation rate ω for SST modification of k-ω are obtained from the following transport equations [10]

$$\frac{\partial}{\partial t}(\rho k) + \frac{\partial}{\partial x_i}(\rho k u_i) = \frac{\partial}{\partial x_j}\left(\Gamma_k \frac{\partial k}{\partial x_j}\right) + \widetilde{G_k} - Y_k + S_k \text{ and} \quad (7)$$

$$\frac{\partial}{\partial t}(\rho \omega) + \frac{\partial}{\partial x_i}(\rho \omega u_i) = \frac{\partial}{\partial x_j}\left(\Gamma_k \frac{\partial \omega}{\partial x_j}\right) + G_\omega - Y_\omega + S_\omega + D_\omega . \quad (8)$$

In these equations $\widetilde{G_k}$represents the production of turbulence kinetic energy due to mean velocity gradients,

calculated as:

$$\widetilde{G}_k = -\rho\overline{u'_i u'_j}\frac{\partial u_j}{\partial x_i} \text{ and} \quad (9)$$

G_ω represents the generation ofω, calculated as:

$$G_\omega = \propto \frac{\omega}{k} G_k. \quad (10)$$

In the high-Reynolds-number form of the $k-\omega$ model

$$\alpha = \alpha_\infty = 1\ . \quad (11)$$

Further in equations (1),Y_k and represent the dissipation of k due to turbulence, calculated as

$$Y_k = \rho\beta^* f_{\beta^*} k, \text{ where} \quad (12)$$

$$f_{\beta^*} = 1. \quad (13)$$

Thus,

$$Y_k = \rho\beta^* k\omega, \text{ where} \quad (14)$$

$$\beta^* = \beta_i^*[1 + \varsigma^* F(M_t)], \text{ where} \quad (15)$$

$$\beta_i^* = \beta_\infty^* \left(\frac{\frac{4}{15} + \left(\frac{Re_t}{R_\beta}\right)^4}{1 + \left(\frac{Re_t}{R_\beta}\right)^4} \right) \quad (16)$$

In the high-Reynolds-number flows

$$\beta_i^* = \beta_\infty^*\ . \quad (17)$$

In the equation (13), $F(M_t)$ represents compressibility correction. This is important member as the supersonic flows must include compressibility effects. Compressibility correction is defined as

$$F(M_t) = \begin{cases} 0 & M_t \le M_{t0} \\ M_t^2 - M_{t0}^2 & M_t > M_{t0} \end{cases}, \text{ where} \quad (18)$$

$$M_t^2 = \frac{2k}{\kappa RT} \quad (19)$$

This yields, that in low-turbulent-kinetic-energy regions the compressibility correction is not applied. In supersonic flow we expect$M_t > M_{t0}$.The ω-dissipation term Y_ω in equation (6) is defined as

$$Y_\omega = \rho\beta f_\beta \omega^2, \text{ where} \quad (20)$$

$$f_\beta = 1. \quad (21)$$

Thus,

$$Y_\omega = \rho\beta\omega^2, \text{ where} \quad (22)$$

$$\beta_i = F_1\beta_{i,1} + (1 - F_1)\beta_{i,2}, \text{ where} \quad (23)$$

$$F_1 = tanh(\Phi_1^4), \text{ where} \quad (24)$$

$$\Phi_1 = min\left[max\left(\frac{\sqrt{k}}{0.09\omega y}, \frac{500\mu}{\varrho y^2\omega}\right), \frac{4\rho k}{\sigma_{\omega,2} D_\omega^+ y^2}\right], \text{ where} \quad (25)$$

$$D_\omega^+ = \left[2\rho\frac{1}{\sigma_{\omega,2}}\frac{1}{\omega}\frac{\partial k}{\partial x_j}\frac{\partial \omega}{\partial x_j}, 10^{-10}\right]. \quad (26)$$

The SST $k-\omega$ model is based on both the standard $k-\omega$model and standard $k-\epsilon$. To blend these models together, the standard $k-\epsilon$ model has been transformed into equations based on $k$and ω. This leads to the introduction of cross-diffusion term defined as

$$D_\omega = 2(1 - F_1)\varrho\sigma_{\omega,2}\frac{1}{\omega}\frac{\partial k}{\partial x_j}\frac{\partial \omega}{\partial x_j} \quad (27)$$

From the above analysis of $k-\omega$ SST model we can find model constants and their likely values in supersonic flows empirically established in past. These constants are summarized in the Table 1 [11].

TABLE I
$k-\omega SST$ MODEL CONSTANTS

Symbols	Values	Symbols	Values
$\sigma_{k,1}$	1.176	α_∞	1
$\sigma_{\omega,1}$	2.0	α_0	1/9
$\sigma_{k,2}$	1.0	β_∞^*	0.09
$\sigma_{\omega,2}$	1.168	R_β	8
a_1	0.31	R_k	6
$\beta_{i,1}$	0.075	R_ω	2.95
$\beta_{i,2}$	0.0828	ζ^*	1.5
α_∞^*	1	M_{t0}	0.25

V. RESULTS

There is a brief example of experimental Schlieren picture taken on initial ejector design. This picture was used to validate the solver setting. We have used the Schlieren picture for validation of turbulent models more complexly in previous work [6].

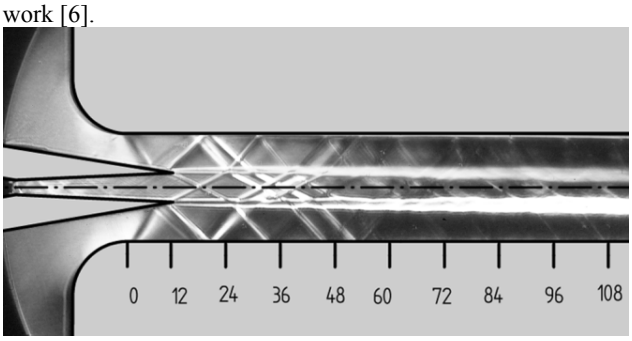

Fig. 8 Schlieren picture of the supersonic ejector in operation. Design regime. p_{01} = 175 kPa,. $p_{exit} = -77\ kPa$.

Direct matching with computed Mach number flow field can be done with the aim of the Fig.8 and 9. Results of pneumatic measurements on the ejector's mixing chamber wall are provided in the Fig10. Good agreement was proved.

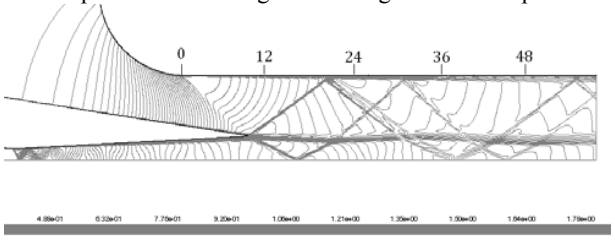

Fig. 9 Contours of computed Mach number. Design regime

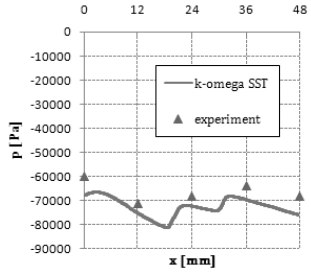

Fig. 10 Static pressure at mixing chamber wall.Matching of the experiment and numerical simulation

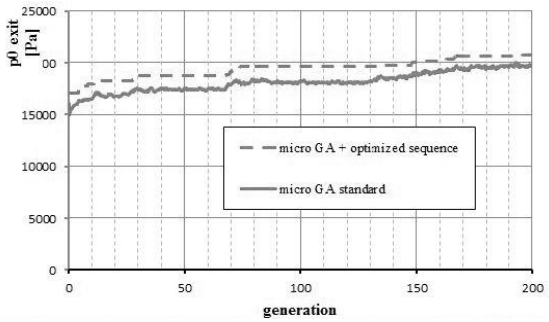

Fig. 11 Generation average total pressure in mixing chamber exit.Matching of the standard micro-GA and GA with optimized sequence

As can be seen from the Fig.11very slow improvement were gained for both standard and newly formed routine. This is mainly due to physical base of the problem. In direct matching the optimized sequence proved faster convergence to the optimum although it was not expected. This was probably caused by more sufficient initialization of the problem. Initialization is done by pseudo-random code based on PC system time. We can recognize rapid improvement during first generations in compare to standard GA and nearly identic trends later on. It is planned to repeat this optimization later to get more results for statistic evaluation.

More significant difference can be found when matching the computational time needed for four-core 3GHz PC station to gain improvement of 5 kPa in the Fig. 11. Final time required by GA with adapted sequence is less than one third of standard routine. The time needed for CFD simulations itself is even 8 hrs lower totally as this time was absorbed by GA to optimize sequences. Lower total count of generation for adaptive GA is caused by faster improvement of objective when compare to standard GA. 5 kPa pressure increase was gained about 30 generations earlier.

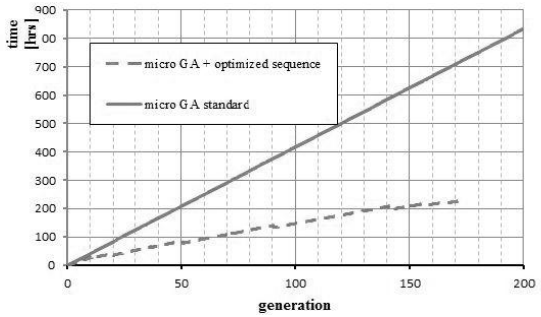

Fig. 12 Overall computational time to reach required improvement of p_{0exit}= 5 KPa

ACKNOWLEDGMENT

Authors would like to thanks to the Czech Science Foundation which supported this work by grant no. P101/10/1709 “Nozzles and diffusers in ejectors” and SGS 2823. The authors thank to Dr. Martin Luxa from Institute of Thermodynamics, Academy of Science of the Czech Republic for help with experimental research.

REFERENCES

[1] Shapiro, A. H. The dynamics and thermodynamics of compressible fluid flow. New York: The Ronald Press Company, 1953.
[2] Moeckel, W. E.Interaction of oblique shock waves with regions of variable pressure, entropy and energy. Washington: NACA, 1952. TN 2725.
[3] Kolář, J. and Šafařík, P.“Interaction of oblique shock wave with shear layer.”In Proceedings of the International Conference XXVII: Meeting of Departments of Fluid Mechanics and Thermomechanics. Plzeň, 2008. pp. 163-170.
[4] Dvořák, V. and Kolář, J.“Shape optimization of supersonic ejectors with several primary nozzles,”in the 2nd International Conference on Engineering Optimization, Lisboa, 6.-9. September 2010.
[5] Dvořák, V.“Shape optimization of supersonic ejector for supersonic wind tunnel.”s.l. : In.: Applied and Computational Mechanics, 2010. pp. 15-24.
[6] Breitkopf, P. and Coelho, R. F.Multidisciplinary design optimization in computational mechanics.s.l. : Wiley-ISTE, 2010.
[7] Hynek, J.Genetic algorithms and genetic programing (in Czech). Prague :Grada Publishing ,a. s., 2008.
[8] Holland, J. H.Adaption in natural and artificial systems.Ann Arbor, Michigan : The University of Michigan Press, 1975.
[9] Zelinka, I. et al.Evolutionary computational techniques (in Czech). Prague : BEN-technickáliteratura, 2008.
[10] Yanagisawa, Y., Akahani, J. and Satoh, T.“Shape-based similarity query for trajectories of mobile objects.”, in Proceedings of Mobile Data Management, Tapei,p. 63-77, 2003.
[11] Wilcox, D.Reassessment of the scale determining equation for advanced turbulent models.1988. AIAA J. 26 (11), 1299-1310.
[12] Menter, F. R. Two-equations Eddy-viscosity turbulence models for engineering applications. 1994. AIAA J. 32(8), 1598-1605.
[13] Inc., Fluent. Fluent user documentation. Lebanon :s.n., 2006.
[14] Dvořák, V., ”Optimized Axi-symmetric ejector – experimental and numerical investigation,”Liberec ,in Proceedings of Experimental Fluid Mechanics,25. – 27. November. pp 34 – 43., 2009.